Novel zinc- and silicon-phthalocyanines as photosensitizers for photodynamic therapy of cholangiocarcinoma

JACOB SCHMIDT[1], WERONIKA KUZYNIAK[1], JANINE BERKHOLZ[1], GUSTAV STEINEMANN[1], RACHEAL OGBODU[1], BJÖRN HOFFMANN[1], GERALDINE NOUAILLES[2], AYŞE GÜL GÜREK[3], BIANCA NITZSCHE[1] and MICHAEL HÖPFNER[1]

[1]Institute of Physiology, Charité-Universitätsmedizin Berlin; [2]Department of Infectious Diseases and Pulmonary Medicine, Charité-Universitätsmedizin Berlin, Corporate Member of Freie Universität Berlin, Humboldt-Universität zu Berlin, and Berlin Institute of Health, D-10117 Berlin, Germany; [3]Department of Chemistry, Gebze Technical University, Gebze, Kocaeli 41400, Turkey

Received October 17, 2017; Accepted March 9, 2018

DOI: 10.3892/ijmm.2018.3620

Abstract. Photodynamic therapy (PDT) has emerged as an effective and minimally invasive cancer treatment modality. In the present study, two novel phthalocyanines, tetra-triethyleneoxysulfonyl substituted zinc phthalocyanine (ZnPc) and dihydroxy-2,9(10),16(17),23(24)-tetrakis(4,7,10-trioxaundecan-1-sulfonyl) silicon phthalocyanine (Pc32), were investigated as photosensitizers (PS) for PDT of cholangiocarcinoma (CC). ZnPc showed a pronounced dose-dependent and predominantly cytoplasmic accumulation in EGI-1 and TFK-1 CC cell lines. Pc32 also accumulated in the CC cells, but this was less pronounced. Without photoactivation, the PS did not exhibit any antiproliferative or cytotoxic effects. Upon photoactivation, ZnPc induced the formation of reactive oxygen species (ROS) and immediate phototoxicity, leading to a dose-dependent decrease in cell proliferation, and an induction of mitochondria-driven apoptosis and cell cycle arrest of EGI-1 and TFK-1 cells. Although photoactivated Pc32 also induced ROS formation in the two cell lines, the extent was less marked, compared with that induced by ZnPc-PDT, and pronounced antipoliferative effects occurred only in the less differentiated EGI-1 cells, whereas the more differentiated TFK-1 cells did not show sustained growth inhibition upon Pc32-PDT induction. *In vivo* examinations on the antiangiogenic potency of the novel PS were performed using chorioallantoic membrane (CAM) assays, which revealed reduced angiogenic sprouting with a concomitant increase in nonperfused regions and degeneration of the vascular network of the CAM following induction with ZnPc-PDT only. The study demonstrated the pronounced antiproliferative and anti-angiogenic potency of ZnPc as a novel PS for PDT, meriting further elucidation as a promising PS for the photodynamic treatment of CC.

Correspondence to: Professor Michael Höpfner, Institute of Physiology, Charité-Universitätsmedizin Berlin, Corporate Member of Freie Universität Berlin, Humboldt-Universität zu Berlin, and Berlin Institute of Health, 1 Charitéplatz, D-10117 Berlin, Germany
E-mail: michael.hoepfner@charite.de

Key words: photodynamic therapy, zinc-phthalocyanine, silicon-phthalocyanine, cholangiocarcinoma, apoptosis, cell cycle, angiogenesis, reactive oxygen species, EGI-1, TFK-1

Introduction

Cholangiocarcinoma (CC) is the second most frequent primary hepatic tumor entity following hepatocellular carcinoma and accounts for 3% of all gastrointestinal tumors (1-3). This aggressive tumor has a poor 5-year-survival rate of 5-10%. CC can be classified into the extrahepatic subtype, which comprises 75% of all cases, and the intrahepatic subtype comprising the remaining 25% (4). Due to the late and unspecific appearance of clinical symptoms, mostly presenting through biliary obstruction, CC is often diagnosed in advanced tumor stages, and ~80% of patients are unsuitable for surgical R0-resection, which currently represents the only curative treatment modality (5-7). Unfortunately, palliative treatment options, including R1/R2-resection, chemotherapy or radiotherapy, show relatively poor results in prolonging the survival rates of the patients. Often, they even lower the patients' quality of life (QoL) due to severe adverse effects (1,7,8). The current standard in palliative management of patients with advanced CC is biliary decompression and relief of obstruction by biliary drainage and stent insertion (9). However, compared with a median survival rate of 3 months without any intervention, for patients treated with biliary drainage, the median survival rate is only 4-10 months (7). In the context of the poor prognosis for patients with non-resectable CC, there is an urgent requirement to develop novel and favorable palliative treatment strategies with high patient tolerability and improved outcome. Photodynamic therapy (PDT) is a novel and non-to-minimally invasive treatment option for several premalignant and malignant diseases, including various forms of gastrointestinal cancer. PDT involves the application and

tumor-specific accumulation of a photosensitizing drug, and its subsequent activation with light of a specific wavelength. In the presence of molecular oxygen, the activation of the PS leads to the generation of reactive oxygen species (ROS), which damage the neoplastic tissue and cause apoptotic and/or necrotic cell death (10). As a tumor-specific ablative method with few adverse effects and no formation of resistance on repetition, unlike that following chemotherapy, PDT offers novel perspectives for the palliative treatment of advanced CC. Randomized controlled trials have demonstrated that PDT alone or in combination with stenting significantly improved the survival rates and QoL of patients with non-resectable CC (6,8,11-15). Ortner *et al* (6) showed that PDT combined with stenting increased the median survival rate of patients with non-resectable CC from 3.3 months (biliary stent treatment alone) to 16.4 months (combined treatment of stenting and PDT). Therefore, PDT may represent a promising strategy for improved palliative treatment of advanced and non-resectable CC (16).

The efficacy of PDT is particularly dependent on the quality of the PS used (17), therefore, there is a constant need for further development of photosensitizers with improved efficacy. Phthalocyanines (Pcs) belong to second generation of photosensitizers and are structurally related to porphyrins, which have been well known as PS for several years (18-20). In particular, metallophthalocyanines bearing a zinc, silicon, aluminum or indium as a central metal atom offer favorable properties for an ideal PS (21). In addition to being photostable, Pc-compounds show a high efficacy in producing ROS upon illumination (20). The high absorption peak of Pcs between 600 and 800 nm allows deep tissue penetration of up to 6-8 mm when photoactivating Pcs with red to deep red light (22,23). Pcs have been shown to preferentially accumulate in malignant tissue and show high retention in tumor cells (24,25). In addition, Pcs do not cause cytotoxic effects in a non-illuminated state (26). In the present study, the antitumor effects and suitability of two novel phthalocyanines: Tetra-triethyleneoxysulfonyl substituted zinc phthalocyanine (ZnPc) and dihydroxy-2,9(10),16(17),23(24)-tetrakis(4,7,10-trioxaundecan-1-sulfonyl) silicon phthalocyanine (Pc32) were investigated as PS for PDT of CC.

Materials and methods

Compounds. ZnPc and Pc32 were prepared by minor modification to the procedures described previously (27). The compounds were dissolved in DMSO of spectroscopic grade (Sigma-Aldrich; Merck KGaA, Darmstadt, Germany). The concentrations of stock solutions were calculated by measuring their optical density at 694 nm with a UV/Vis spectrometer (Ultraspec 2100; GE Healthcare Life Sciences, Chalfont, UK) and based on the Lambert-Beer relationship with $\varepsilon_{694\ nm} = 2.04x10^5\ M^{-1}\ cm^{-1}$ (ZnPC) or by measuring the compounds weight with a microbalance (Sartorius AG, Göttingen, Germany) and based on the molar solution concentration equation: Molarity (mol/l) = mass (g)/volume (l) x[1/molecular weight (g/mol)] (Pc32). ZnPc and Pc32 were donated by the Department of Chemistry, Gebze Institute of Technology (Gebze, Turkey). The stock solutions were prepared at concentration of 15-25 mM. Working solutions (0.2-10 μM) were made up in medium so that the DMSO concentration never exceeded 0.25%.

Cell culture. The poorly differentiated EGI-1 CC cell line (Leibnitz Institute DSMZ, Braunschweig, Germany; no. ACC385) (28), and the partly papillary and partly tubular TFK-1 CC cell line (Leibnitz Institute DSMZ, no. ACC344) (29) were derived from patients with extrahepatic bile tract carcinoma, which had not been exposed to chemotherapy or radiotherapy. The two cell lines were cultured in RPMI 1640 medium (Gibco; Thermo Fisher Scientific, Inc., Waltham, MA, USA), supplemented with 100 ml/l fetal calf serum (FCS; Biochrom AG, Berlin, Germany), 100 U/ml penicillin, 100 μg/ml streptomycin and 2 mM L-glutamine (both from Biochrom AG, Berlin, Germany). The cells were maintained under 37˚C in a humidified atmosphere containing 5% CO_2. The culture medium was replaced every second day, and once a week the cells were passaged using 1% trypsin/EDTA.

Light source and irradiation. Irradiation of the cancer cells was performed with a broad-band light source equipped with a 100-W halogen lamp (EFR 12 V/100 W GZ -6.35 lamp Omnilux; Thomann GmbH, Burgebrach, Germany) with a spectral output of 400-800 nm. The optimal conditions for PDT treatment were reached at a cell density of 70-80% monolayer-confluence in the respective plastic dishes used for the examinations. To prevent infrared irradiation, a heat-reflecting filter cutting off wavelengths of ≥700 nm was embedded in the optical path. The illuminated area (5.5x4.5 cm) had an average power density of 80 W/m^2. The light energy dose was measured with a P-9710 radiometer controlled by a silicon photocell (Optometer P 9710 Gigahertz-Optik (Munich, Germany). The total light energy dose was calculated by integrating the energy signal over the entire period of irradiation (25).

PDT treatment. For PDT treatment, the cells were seeded and cultivated in an experiment-dependent number and subsequently incubated for 10-24 h with ZnPc (0.2-10 μM) or Pc32 (1-10 μM) in the dark at 37˚C in a humidified atmosphere containing 5% CO_2. For the measurement of growth inhibition $1.5x10^3$ EGI-1 cells, and $1x10^3$ TFK-1 cells per 100-μl well were seeded in 96-well microtiter plates and cultivated for 48 h prior to incubation with the PS. For the determination of cytotoxicity, the cells were seeded at a density of $2.5x10^4$ cells/100 μl well in a 96-well microtiter plate. Following the incubation period, the PS-containing medium was replaced with PBS, and the cells were irradiated with 10 J/cm^2. The temperature during irradiation was measured with a digital thermometer placed inside of the irradiation system and did not exceed 37˚C. Following irradiation, the PBS was replaced with PS-free medium and the cells were incubated at 37˚C with 5% CO_2 in a humidified atmosphere for another 24-96 h. 'Dark controls' were treated in the same manner, with a PS-incubation period of 24 h, but without subsequent photoactivation by PDT. Dark controls were included to determine the cytotoxic effects of the PS in the absence of light for 24-72 h (25).

Measurement of growth inhibition. The PDT-induced changes in the number of CC cells were determined by crystal violet staining of cellular DNA, as described previously (30). In brief,

the cells were fixed with 1% glutaraldehyde and stained with 0.1% crystal violet. The unbound dye was removed by washing with water. The DNA-bound crystal violet was solubilized with 0.2% Triton X-100 in PBS. Light extinction, which increases linearly with cell number, was analyzed at 570 nm using an ELISA reader.

Intracellular uptake and accumulation. The cells were cultured on glass cover slips and incubated with increasing concentrations of ZnPc (0.2-5 μM) and Pc32 (1-10 μM). Following incubation for 24 h, the cells were washed with PBS and fixed for at least 30 min at -20˚C in methanol. The intracellular distribution of ZnPc was analyzed by measuring its fluorescence with a confocal laser microscope (Leica DMI 6000; Leica Microsystems GmbH, Wetzlar, Germany) with an excitation HeNe laser (700 nm) and detection of PMT at 400-800 nm, performed with a x63 glycerin immersion objective. Digital images were processed using Leica LAS AF Lite software (version 3.2.0; Leica Microsystems GmbH).

Determination of cytotoxicity. The PDT-induced cytotoxicity was determined by measuring the release of lactate dehydrogenase (LDH) from the cytosol of the damaged cells into the supernatant (Cytotoxicity Detection KitPLUS LDH; cat. no. 04744926001; Roche Diagnostics GmbH, Mannheim, Germany) (31). Following PDT treatment, cells incubated with 1% Triton X-100 served as a control for maximum LDH release. Following PDT, the supernatant was transferred to fresh plates and mixed with catalyst and dye solution for 30 min, resulting in the formation of formazan dye proportional to LDH enzyme activity. The absorbance was measured at 490/630 nm using an ELISA reader (Dynex Technologies, Denkendorf, Germany) and cytotoxicity was determined by calculating the percentage of LDH release in the treated sample, compared with the LDH release of the untreated cells, the value of which was 0%, and the maximum LDH release of the Triton X-100 lysed cells, the value of which represented 100% (32). All experiments were performed in triplicate.

Measurement of apoptosis-specific caspase-3 activity. Changes in caspase-3 activity were measured from the cleavage of the fluorogenic substrate AC-DEVD-AMC (EMD Millipore, Billerica, MA, USA), as described previously (32). At 8 and 24 h post-PDT, the cells were harvested and lysed with lysis buffer. Subsequently, the lysates were incubated for 1 h at 37˚C with a substrate solution containing 20 μg/ml AC-DEVD-AMC, 20 mM HEPES, 10% glycerol and 2 mM DTT at pH 7.5. Substrate cleavage was measured fluorometrically using a VersaFluor fluorometer (Bio-Rad Laboratories, Inc., Hercules, CA, USA; filter sets: ex 360/40 nm, em 460/10 nm). Campthotecin was used as a positive control.

Western blot analysis. Western blot analysis was performed as described previously (33). Briefly, whole-cell extracts were prepared by lysing the cells in RIPA buffer. Protein concentration of the lysates was determined by using bicinchoninic acid protein assay kit (Thermo Fisher Scientific, Inc.) and ≤20 μg protein were subjected to gel electrophoresis with 10 or 12% gels and then transferred onto a PVDF membrane by electroblotting for 1.5 h. Following blocking in 5% skim milk powder solution (Merck Millipore) for at least 1 h, the blots were incubated with primary antibodies at 4˚C overnight. The antibodies were directed against B-cell lymphoma 2 (Bcl-2)-associated X protein (Bax 1:1,000; sc-493), extracllular signal-regulated kinase (ERK)1/2 (1:1,000; sc-94), GAPDH (1:1,000; sc-25778), Cyclin D1 (1:1,000; sc-8396) and Cyclin B1 (1:1,000; sc-752) from Santa Cruz Biotechnology, Inc. (Santa Cruz, CA, USA), and Bcl-2 (1:1,000; B3170) and β-actin (1:2,000; A5441) from Sigma-Aldrich; Merck KGaA, Darmstadt, Germany). Following incubation with horseradish peroxidase-coupled anti-IgG antibodies (1:10,000; NA931V and NA934V; GE Healthcare Life Sciences) at room temperature for at least 1 h, the blots were developed using enhanced chemiluminescent detection (ECL Clarity Max; Bio-Rad Laboratories, Inc., Hercules, CA, USA) and processed with Chemiluminescence Imager Celvin® S 420 (Biostep, Burkhardsdorf, Germany). Relative changes in the expression of Bax, Cyclin D1, Cyclin B1 and ERK1/2 of the PDT-treated, vs. untreated control cells were measured densitometrically using ImageJ software (version 2.0.0-rc-43/1.50e; National Institutes of Health, Bethesda, MD, USA). Protein expression was normalized to housekeeping gene expression of β-actin or GAPDH. The protein level of untreated and housekeeping gene-normalized cells was set as 1. Values >1 indicated upregulation and values <1 indicated downregulation of a respective protein expression.

Measurement of ROS. The cells were incubated with ZnPc and Pc32 for 24 h and then illuminated with 10 J/cm^2. ROS formation was determined 2 and 7 h post-PDT for ZnPc and 2 h post-PDT for Pc32 using CellROX Green and CellROX Orange (Thermo Fisher Scientific, Inc.) according to the manufacturer's protocol. Controls underwent PDT without previous ZnPc loading. The cells were analyzed using a fluorescence microscope (Axioskop 40, Zeiss; x40 objective, 1.30 NA; Carl Zeiss AG, Oberkochen, Germany) equipped with a digital camera (DX4-285FW, Kappa Optronics (Gleichen, Germany). CellROX Green depicts ROS formation in the nucleus and mitochondria (ex/em approximately 470/525 nm) by producing bright green fluorescence, whereas orange fluorescence (CellROX Orange) depicts ROS in the cytoplasm of the cells (ex/em approximately 546/575 nm).

Cell cycle analysis by flow cytometry (FACS). At 24 h post-PDT-treatment (10 J/cm^2), the cells were washed with PBS and fixed in ice-cold ethanol at -20˚C. Following incubation for at least 30 min, the ethanol was removed by centrifugation (273.4 x g at 4˚C for 4 min) and the cell pellets were washed twice in PBS. The cell pellets were resuspended in PBS containing 40 μg RNase-A and incubated for 30 min at 37˚C. Subsequently, the cells were pelleted (241.3 x g at 4˚C) again and resuspended in PBS containing 50 μg/ml propidium iodide. Then cells were analyzed using the FACSCanto II analyzer (BD Biosciences, Franklin Lakes, NJ, USA) and FCS Express 6 software (De Novo Software, Los Angeles, CA, USA). Corresponding to their phase-specific DNA-content, the cells were divided into G1, S, G2/M phases and, when present, the sub-G1 phase which was interpreted as apoptotic.

Determination of antiangiogenic effects using a chorioallantoic membrane (CAM) assay. The CAM assay was performed as described in a previous study (34). In brief, fertilized chicken eggs (Lohmann Tierzucht, Cuxhaven, Germany) were bred in an incubator at 37˚C in constant humidity for 3 days. After 3 days, a square window was cut into the shell of each egg to assure a living embryo and allow detachment of the developing CAM from the shell. The window was sealed and the eggs were incubated for additional 7 days. On day 10, the tapes were removed and two small silicone rings were placed onto the CAM, and either 20 μl of vehicle (negative control), ZnPc (10 μM) or Pc32 (10 μM) were topically applied. The eggs were then sealed and incubated in the dark at 37˚C in a humidified incubator. After 24 h, the treated areas were illuminated with 10 J/cm^2. Changes in the microvasculature of the CAM were examined 24 h post-PDT and *in vivo* images were captured using a stereomicroscope equipped with a digital camera (Di-Li, Kaiserslautern, Germany).

Statistical analysis. Unless stated otherwise, data are presented as the mean ± standard deviation. Significance between values was analyzed with GraphPad Prism 6 software (GraphPad Software, Inc., La Jolla, CA, USA) using an unpaired t-test. $P<0.05$ was considered to indicate a statistically significant difference.

Results

Photosensitizer uptake and intracellular accumulation. The intracellular uptake and accumulation of ZnPc and Pc32 were investigated using confocal laser scanning microscopy. Following incubation for 24 h with non-photoactivated ZnPc, the EGI-1 and TFK-1 cells showed a dose-dependent uptake and predominantly cytoplasmic accumulation (Fig. 1A). By contrast, the uptake of Pc32 was comparably lower; even at 10 μM, only a marginal to moderate cytoplasmic accumulation was observed (Fig. 1B).

Growth inhibition of photoactivated and non-photoactivated ZnPc and Pc32. The optimal loading time prior to the PDT was investigated in TFK-1 and EGI-1 cells following incubation with increasing concentrations of ZnPc (0.2-5 μM) for 10, 16 and 24 h, and analyzed using crystal violet staining. The 'dark toxic' effects of non-photoactivated ZnPc (2.5-10 μM) and the antiproliferative effect of non- and photoactivated Pc32 (1-10 μM) were investigated following prior to incubation for 24 h and subsequently analyzed using crystal violet staining.

Preloading of ZnPc for 10 h was sufficient to elicit pronounced PDT-induced growth inhibitory effects. However, a further increase in the preloading time of up to 24 h increased the antiproliferative effectiveness of PDT in the two cell lines (Fig. 1C and D). Based on these findings, the subsequent investigations were performed following a preloading period of 24 h of the respective PS. Incubation with non-photoactivated ZnPc or Pc32 (dark toxicity) for 24 h did not affect the proliferation of either CC cell lines at any time point. Even the high 10 μM concentration of ZnPc or Pc32 did not induce any appreciable antiproliferative effects, showing that neither phthalocyanines were toxic in the absence of light (Fig. 2A and B).

The growth inhibitory effects of PDT with ZnPc (0.2-10 μM) and Pc32 (1-10 μM) were determined using crystal violet staining. In the two cell lines, light activated ZnPc-PDT led to pronounced time- and dose-dependent growth inhibition. The IC_{50} values of ZnPc-PDT of EGI-1 and TFK-1 were 0.5±0.17 and 1.7±0.13 μM, respectively, as determined 24 h post-PDT. Compared with the TFK-1 cells, the response of the EGI-1 cells was more pronounced. However, in both cell lines, an overall decrease of ≥90% was observed, and there were no signs of re-proliferation of cells that evaded immediate PDT-induced death at moderate ZnPc-doses (1-2.5 μM) (Fig. 2A and B). The effect of ZnPc-PDT on the expression of ERK1/2, which is involved in cell growth, differentiation and proliferation, was also evaluated by western blot analysis. ZnPc-PDT led to a decrease in the expression of ERK1/2 in the EGI-1 and TFK-1 cells in a dose-dependent manner (Fig. 2C and D).

Pc32-PDT (1-10 μM) induced a sustained time- and dose-dependent decrease in the proliferation of EGI-1 cells (Fig. 3A), but did not induce pronounced antiproliferative effects in the TFK-1 cells. Pc32-PDT was not able to stop the re-proliferation of TFK-1 cells that evaded immediate PDT-induced cell death (Fig. 3B). As described for ZnPc above, incubation with non-photoactivated Pc32 (dark toxicity) did not affect the proliferation of either CC cell lines at any time point. Even the high 10 μM concentration of Pc32 did not induce any appreciable antiproliferative effects, showing that the Pc32 phthalocyanine was not cytotoxic in the absence of light (Fig. 3).

Induction of ROS formation. ZnPc- and Pc32-PDT-induced ROS generation was analyzed using fluorogenic dyes, which are sensitive for cytoplasmic (orange) or mitochondrial/nuclear (green) ROS and subsequent fluorescence microscopy. Compared with the control (Fig. 4A), at 2 h post-ZnPc-PDT, a marked dose-dependent increase in ROS formation was observed in the cytoplasm and the mitochondria/nucleus of the EGI-1 cells (Fig. 4B). Even at low ZnPc-concentrations of 0.5 μM, marked generation of ROS was observed in the cytoplasm and mitochondria/nuclei (data not shown). However, despite the dose-dependent increase in overall ROS formation, there was no preferred localization of ROS in either the nucleus/mitochondria or the cytoplasm. By contrast, 2 h following Pc32-PDT, a comparably lower increase of ROS formation was observed in the EGI-1 cells (Fig. 4C). This finding was in accordance with the reduced uptake and limited antiproliferative effects of Pc32 shown in the prior experiments. The same pattern of results was observed for the TFK-1 cells following exposure to ZnPc-PDT, compared with the control (Fig. 4D and E), even at a low concentration of 1.7 μM (data not shown), and following exposure to Pc32-PDT (Fig. 4F).

Evaluation of immediate cytotoxicity following exposure to PDT with ZnPc and Pc32. The immediate cytotoxic effects of photoactivated ZnPc in TFK-1 and EGI-1 cells were determined by measuring the LDH release. The leakage of intracellular LDH into the culture medium is an indicator of ROS-induced cytotoxicity due to a damage of the integrity of the membrane of cells or cell organelles, including mitochondria, golgi vesicles and nuclei. In the two cell lines, ZnPc-PDT (0.5-5 μM) resulted in a significant time- and concentration-dependent

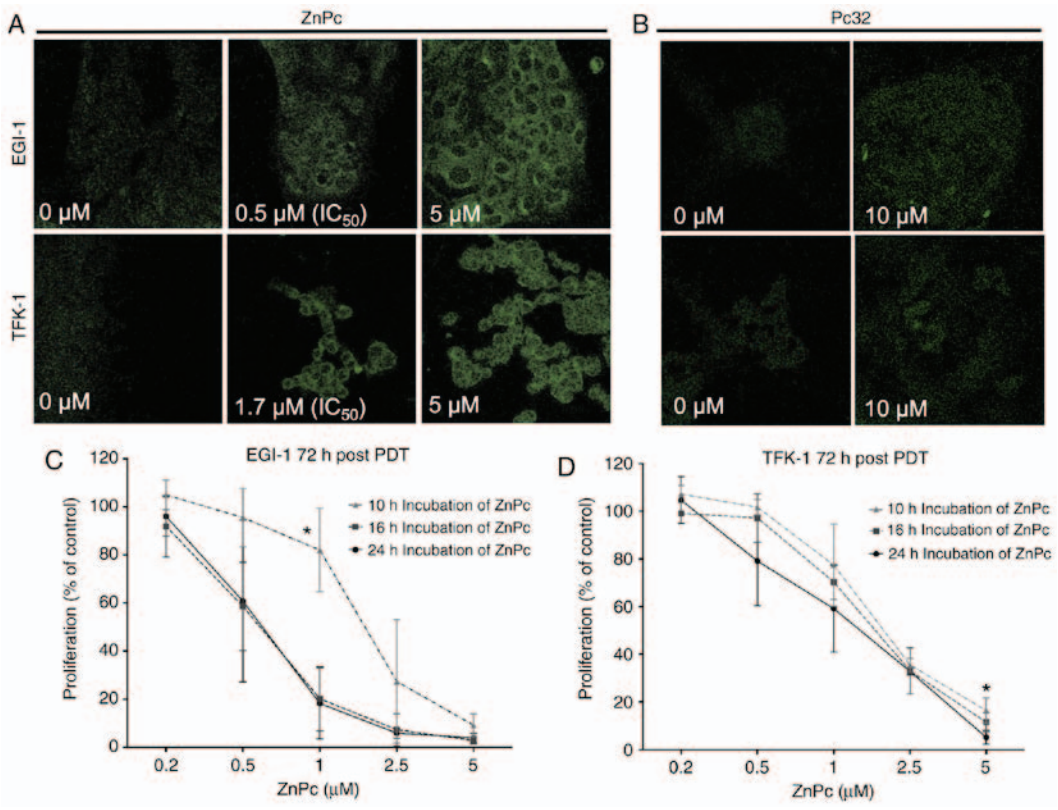

Figure 1. Uptake and loading times of ZnPc and Pc32 in cholangiocarcinoma cells. (A) Dose-dependent uptake and cytoplasmic accumulation of ZnPc in EGI-1 and TFK-1 cells at 24 h, as determined by confocal scanning microscopy (ex/em 700/400-800). (B) Pc32 uptake at the highest concentration of 10 μM following incubation for 24 h. (C) Efficacy of ZnPc-PDT (10 J/cm^2) correlated with the preloading time of the photosensitizer. The longer the loading time, the more pronounced the antiproliferative effect of ZnPc-PDT was in (C) EGI-1 and (D) TFK-1 cells. Results are representative of at least three independent experiments. Magnification, x63. *P<0.05, 10 h incubation, vs. 24 h incubation. ZnPc, tetra-triethyleneoxysulfonyl substituted zinc phthalocyanine; Pc32, dihydroxy-2,9(10),16(17),23(24)-tetrakis(4,7,10-trioxaundecan-1-sulfonyl) silicon phthalocyanine; PDT, photodynamic therapy.

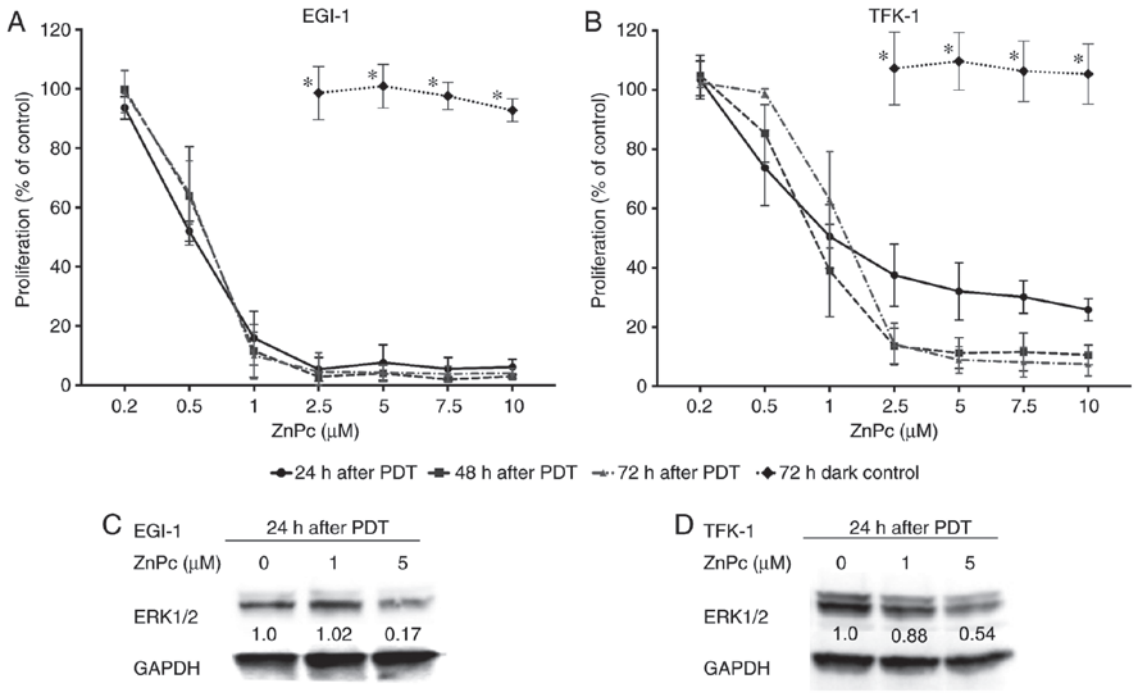

Figure 2. Growth inhibitory effects of ZnPc-PDT in cholangiocarcinoma cells. ZnPc-PDT (10 J/cm^2) dose- and time-dependently decreased the number of (A) EGI-1 and (B) TFK-1 cells of ≥90%. Non-photoactivated ZnPc did not exhibit any appreciable 'dark toxicity' in either cell line. ZnPc-PDT induced a marked decrease in the expression of mitogen-activated protein kinase-pathway related protein ERK1/2 in (C) EGI-1 and (D) TFK-1 cells. Results are representative of at least three independent crystal violet experiments and two western blot experiments. *P<0.05 non-photoactivated, vs. photoactivated ZnPc (72 h-post PDT). ZnPc, tetra-triethyleneoxysulfonyl substituted zinc phthalocyanine; Pc32, dihydroxy-2,9(10),16(17),23(24)-tetrakis(4,7,10-trioxaundecan-1-sulfonyl) silicon phthalocyanine; PDT, photodynamic therapy; ERK1/2, extracellular signal-regulated kinase 1/2.

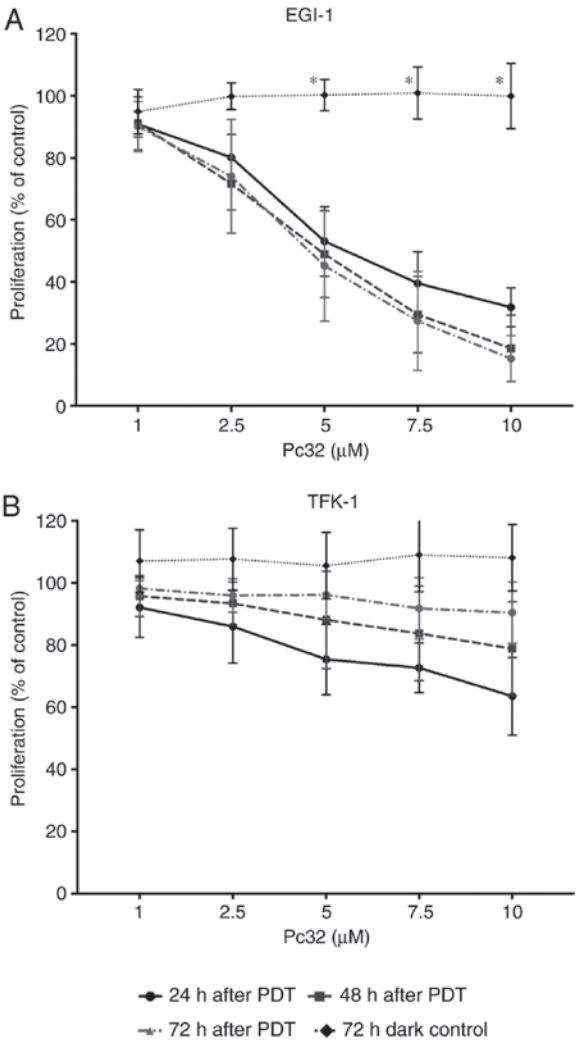

Figure 3. Growth inhibitory effects of Pc32-PDT in cholangiocarcinoma cell lines. (A) Pc32-PDT (10 J/cm^2) led to a time- and dose-dependent decrease in the proliferation of EGI-1 cells. (B) In TFK-1 cells, Pc32-PDT did not induce marked or sustained growth inhibition. Findings of at least three independent experiments are shown. *P<0.05 non-photoactivated vs. photoactivated Pc32 post PDT. ZnPc, tetra-triethyleneoxysulfonyl substituted zinc phthalocyanine; Pc32, dihydroxy-2,9(10),16(17),23(24)-tetrakis(4,7,10-trioxaundecan-1-sulfonyl) silicon phthalocyanine; PDT, photodynamic therapy.

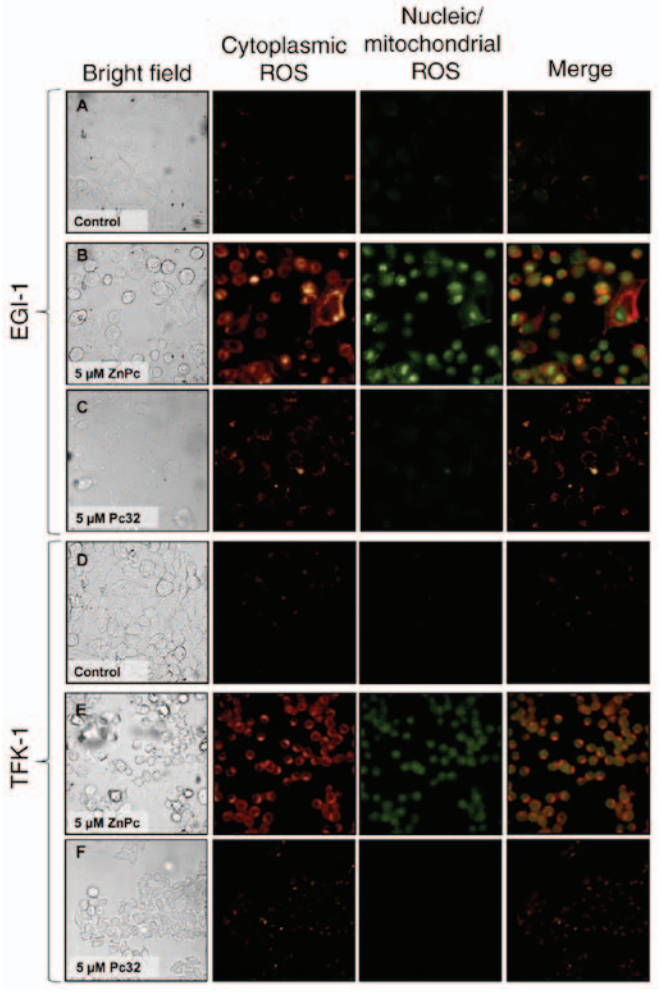

Figure 4. ZnPc- and Pc32-PDT induced formation of ROS in cholangiocarcinoma cells. In EGI-1 cells, compared with the (A) control, at (B) 2 h post-ZnPc-PDT (5 μM/10 J/cm^2), a marked induction of ROS generation was observed in the cytoplasm (orange) and the nucleus/mitochondria (green). (C) At 2 h post-Pc32-PDT (5 μM/10 J/cm^2), minimal induction of ROS formation occurred. In TFK-1 cells, compared with the (D) control, at (E) 2 h post-ZnPc-PDT (5 μM/10 J/cm^2), a marked induction of ROS generation was observed in the cytoplasm (orange) and the nucleus/mitochondria (green). (F) At 2 h post-Pc32-PDT (5 μM/10 J/cm^2), minimal induction of ROS formation occurred. Results are representative of four independent experiments. Magnification, x40. ZnPc, tetra-triethyleneoxysulfonyl substituted zinc phthalocyanine; Pc32, dihydroxy-2,9(10),16(17),23(24)-tetrakis(4,7,10-trioxaundecan-1-sulfonyl) silicon phthalocyanine; PDT, photodynamic therapy; ROS, reactive oxygen species.

increase of immediate cytotoxicity following 1-6 h (Fig. 5). The EGI-1 cells showed a maximum LDH release of 34.8% at 6 h post-PDT (Fig. 5A), whereas the effect was less pronounced in the TFK-1 cells. However, in the TFK-1 cells, an increase in LDH release of ~17.8% became apparent (Fig. 5B), showing the cytotoxic potential of ZnPc for PDT of CC. Compared with these findings, Pc32-PDT (0.5-5 μM) led to only weak immediate cytotoxic effects in the two cell lines. The EGI-cells showed a maximum LDH release of 9.5% at 6 h post-Pc32-PDT (Fig. 5C), whereas a maximum LDH release of 8.5% was measured in the TFK-1 cells (Fig. 5D).

Apoptotic effects of ZnPc-PDT in CC cells. In addition to the induction of necrotic cell death via immediate cytotoxicity, PDT can also lead to apoptosis by ROS-mediated disruption of mitochondrial integrity. Due to the limited growth inhibitory and cytotoxic effects of Pc32-PDT, the possible apoptotic effects were predominantly examined for ZnPc-PDT. The apoptosis-specific activation of caspase-3 was determined at 8 and 24 h post-PDT. In addition, the changes in the proportions of cells in the apoptosis-indicating sub-G1 phase of the cell cycle were elucidated by FACS-analysis. ZnPc-PDT (0.2-5 μM) led to a time- and dose-dependent increase of caspase-3 activity in the EGI-1 and TFK-1 cells of up to 26- and 6-fold, compared with the control cells, which were illuminated but not loaded with ZnPc (Fig. 6A and B). In particular, the induction of capsase-3 activity in the EGI-1 cells occurred rapidly, reaching the highest value at 8 h post-PDT with 5 μM ZnPc (Fig. 6A).

Due to the process of partial DNA-fragmentation (karrhyorexis) and its loss during the formation of apoptotic bodies (35), the two cell lines showed a concentration-dependent increase in the proportion of cells containing sub-G1 phase-specific hypoploide DNA content 24 h post-ZnPc-PDT (Fig. 6C). These

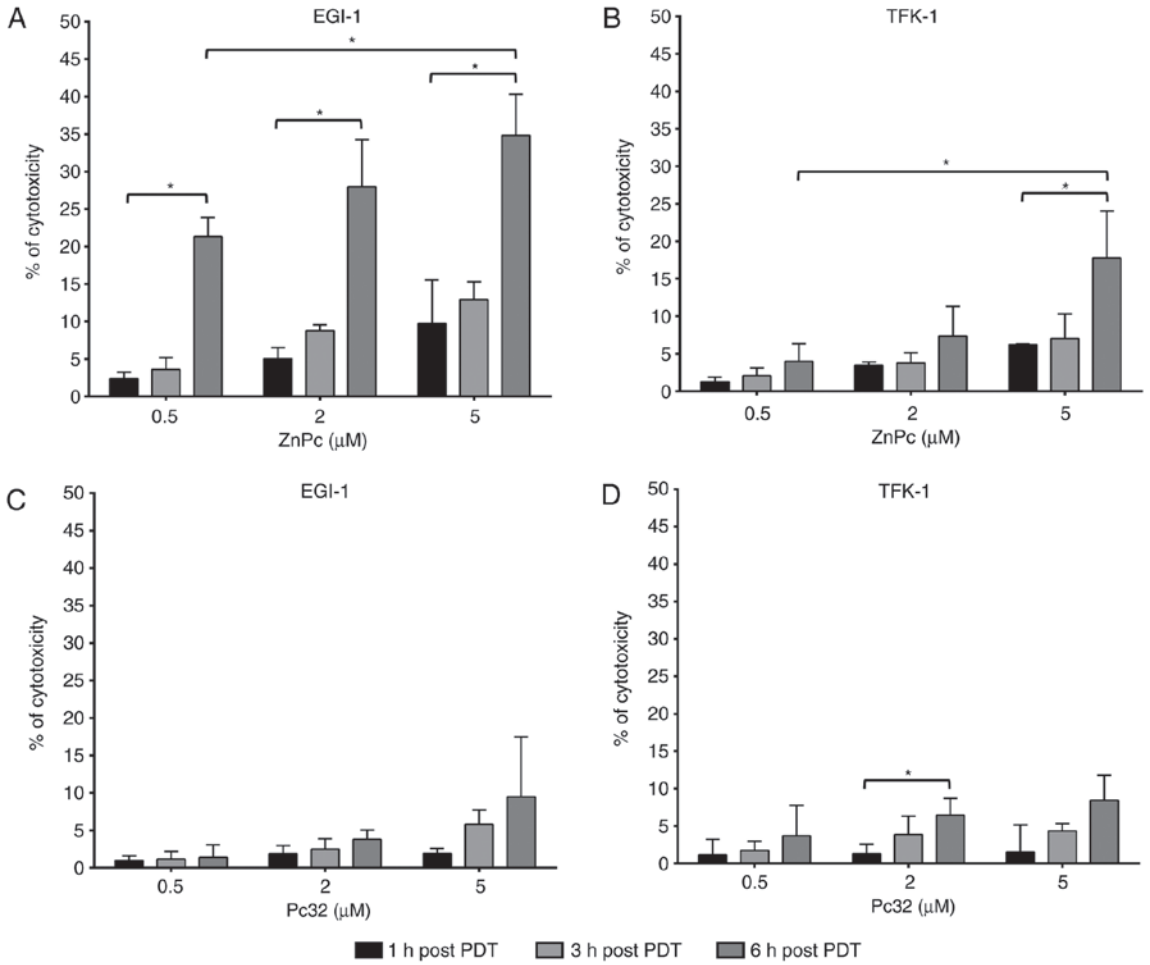

Figure 5. Immediate cytotoxicity of ZnPc- and Pc32-PDT in cholangiocarcinoma cells. ZnPc-PDT (0.5-5 μM/10 J/cm^2) induced a more marked time- and dose-dependent release of cytotoxicity-indicating LDH into the supernatant of (A) EGI-1 and (B) TFK-1 cells, compared with Pc32-PDT (0.5-5 μM/10 J/cm^2) in the (C) EGI-1 and (D) TFK-1 cells. Results are representative of three independent experiments. *P<0.05 cytotoxicity 1 vs. 6 h post-PDT or 0.5 vs. 5 μM 6 h post-PDT. ZnPc, tetra-triethyleneoxysulfonyl substituted zinc phthalocyanine; Pc32, dihydroxy-2,9(10),16(17),23(24)-tetrakis(4,7,10-trioxaundecan-1-sulfonyl) silicon phthalocyanine; PDT, photodynamic therapy; LDH, lactate dehydrogenase.

effects occurred in both cell lines, but were less pronounced in the TFK-1 cells. Compared with the untreated controls, ZnPc-PDT (5 μM, 10 J/cm^2) led to a 5-fold increase in the apoptotic sub-G1 peak, but there was an increase of >18-fold in the EGI-1 cells.

The activity of caspase-3 and changes in sub-G1-phase-specific DNA content can be driven by either intrinsic-mitochondrial or extrinsic apoptotic pathways. To elucidate the induction of apoptosis via one way or the other, the expression of two proteins associated with the mitochondria-driven apoptotic pathway, namely Bax and Bcl-2, were evaluated by western blot analysis. ZnPc-PDT induced a time- and dose-dependent decrease in the protein expression of anti-apoptotic Bcl-2 and a simultaneous increase in the protein expression of pro-apoptotic Bax in the EGI-1 cells at 12 and 24 h post-PDT (Fig. 6D). Compared with the EGI-1 cells, the TFK-1 cells showed a less marked decrease in the expression of Bcl-2, and a less pronounced increase in the expression of Bax, and these effects occurred later (Fig. 6E).

Changes of cell cycle distribution. The effect of ZnPc-PDT on the cell cycle distribution of the EGI-1 and TFK-1 cells was measured by flow cytometry. Additionally, the expression levels of two cell cycle phase-specific proteins Cyclin D1 and Cyclin B1 were evaluated by western blot analysis. At 24 h post-ZnPc-PDT, the EGI-1 cells showed a dose-dependent increase in the number of cells in the G_0/G_1-phase, with a corresponding decrease in the number of cells in the G_2/M-phase (Fig. 7A and B). At 6 and 24 h post-PDT treatment, a corresponding decrease in the expression of cell cycle promoter Cyclin D1, acting at the G_1- to S-phase transition, was observed (Fig. 7C). By contrast, the TFK-1 cells responded with a decrease of cells in the G_0/G_1-phase and a corresponding increase of cells in the G_2/M-phase (Fig. 7D and E). These changes were accompanied by a decrease in the expression of cell cycle promoter Cyclin B1, which is required for the transition of cells from the G_2- to M-phase (Fig. 7F).

Angiogenesis inhibition. The influence of ZnPc and Pc32-PDT on the formation of new blood vessels was evaluated using an angiogenesis assay with the CAM of fertilized chicken eggs (CAM assay). An area of 5 mm in diameter of 10-day old CAMs was incubated with either 10 μM of ZnPc or Pc32 for 24 h and then illuminated (10 J/cm^2). Prior to the PDT treatment, the CAM consisted of a regular vascular network with an intact capillary bed. In the control-treated CAMs,

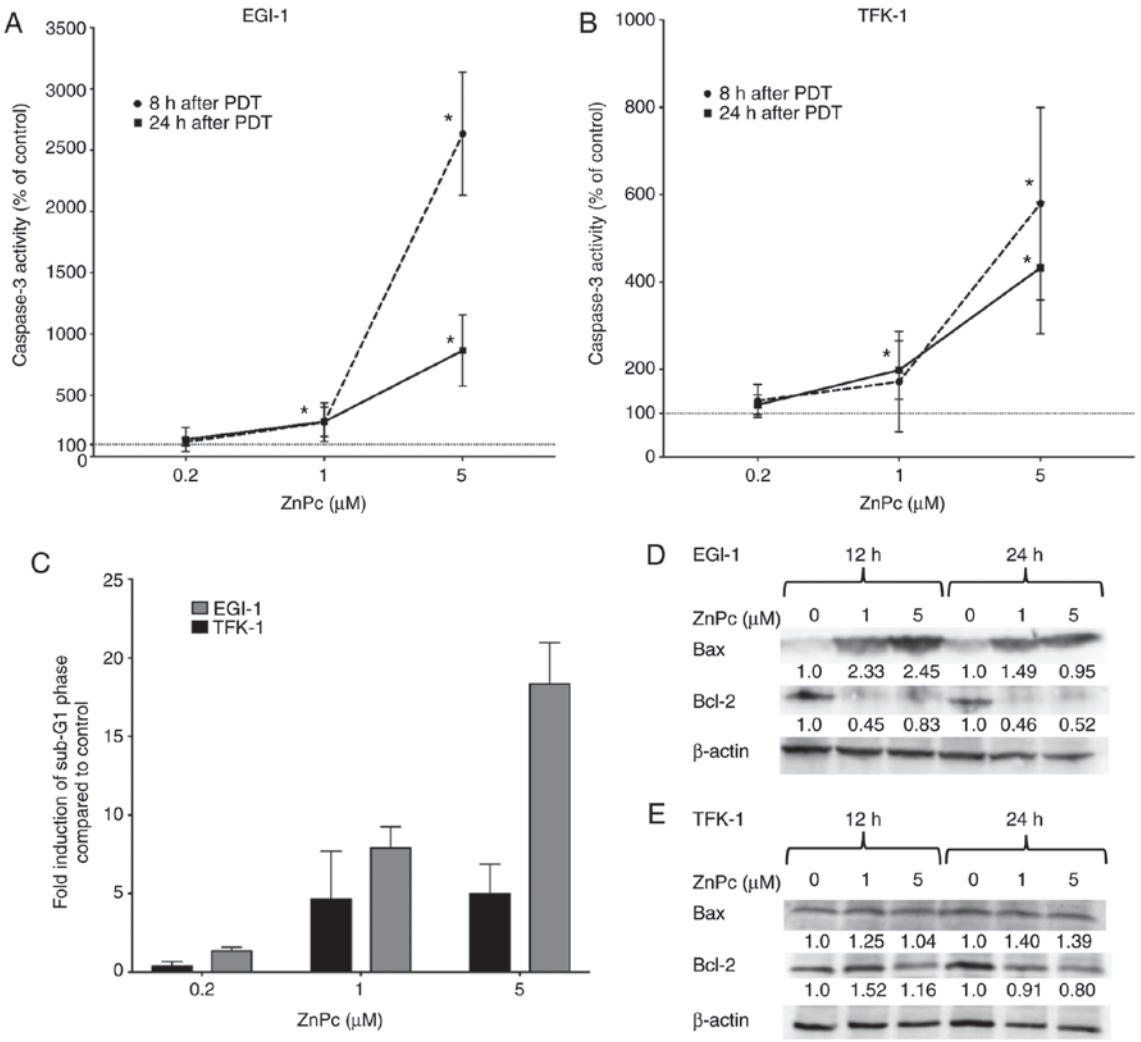

Figure 6. Induction of apoptosis in cholangiocarcinoma cells by ZnPc-PDT. The effector-caspase-3 was measured 8 and 24 h post PDT with ZnPc (0.2-5 μM) in (A) EGI-1 and (B) TFK-1 cells. (C) A dose-dependent increase in the apoptotic subG1-peak was determined by measuring changes in the hypoploide DNA content following ZnPc-PDT treatment in EGI-1 and TFK-1 cells. Western blot analysis of expression of pro-apoptotic Bax and anti-apoptotic Bcl-2 at 12 and 24 h in (D) EGI-1 and (E) TFK-1 cells. Densitometric analysis with ImageJ revealed the relative increase or decrease in the protein expression of pro- and antiapoptotic proteins Bax and Bcl-2 following ZnPc-PDT treatment, normalized to β-actin. Results are representative of at least three independent experiments. *P<0.05 caspase-3 activity 8 or 24 h post-PDT, vs. control. ZnPc, tetra-triethyleneoxysulfonyl substituted zinc phthalocyanine; Pc32, dihydroxy-2,9(10),16(17),23(24)-tetrakis(4,7,10-trioxaundecan-1-sulfonyl) silicon phthalocyanine; PDT, photodynamic therapy; Bcl-2, B-cell lymphoma 2; Bax, Bcl-2-associated X protein.

no changes in the development of the vascular network were observed. There was a constant increase in microvessel formation, as shown in the progression of new branches at the distal end of small vessels (Fig. 8A). Pc32-PDT did not alter the development or distribution of new blood vessels (Fig. 8B). By contrast, ZnPC-PDT induced the degeneration of the existing vascular network, leading to nonperfused regions (Fig. 8C). In addition, changes in the branching of the small supplying vessels became apparent, suggesting avascular and antiangiogenic properties of ZnPc-PDT.

Discussion

Palliative treatment options for CC are disappointing. Patients suffering from advanced CC have a poor prognosis in terms of survival rate and experience a low QoL. Therefore, there is an urgent requirement for novel effective treatment approaches, including PDT. In a previous study ZnPc was proposed as a promising photosensitizer for PDT of gastrointestinal cancer entities, including esophageal and neuroendocrine gastrointestinal carcinoma (25,36). The present study focused on the efficacy and the underlying mechanisms of PDT treatment of CC cells with the two novel metallophthalocyanines, ZnPc and Pc32.

A main requirement for a PS is the absence of cytotoxic effects without photoactivation, or 'dark toxicity', to avoid unwanted side effects and the destruction of healthy tissue (37), whereas the photoactivation of the PS requires a persistent antineoplastic effect on the PDT-treated tumor cells/tissue. In the present study it was shown that neither incubation with non-photoactivated ZnPc, nor with non-photoactivated Pc32 (Fig. 2) led to undesired 'dark toxic' effects on the CC cells.

The photoactivated ZnPc-PDT led to a marked and sustained time- and dose-dependent antiproliferative effect in the two CC cell lines. Correspondingly, a decrease in the expression of the mitogen-activated protein kinase (MAPK)-related protein, ERK1/2, was observed, indicating the downregulation of proliferation-promoting processes, cellular differentiation and survival at a molecular level in the

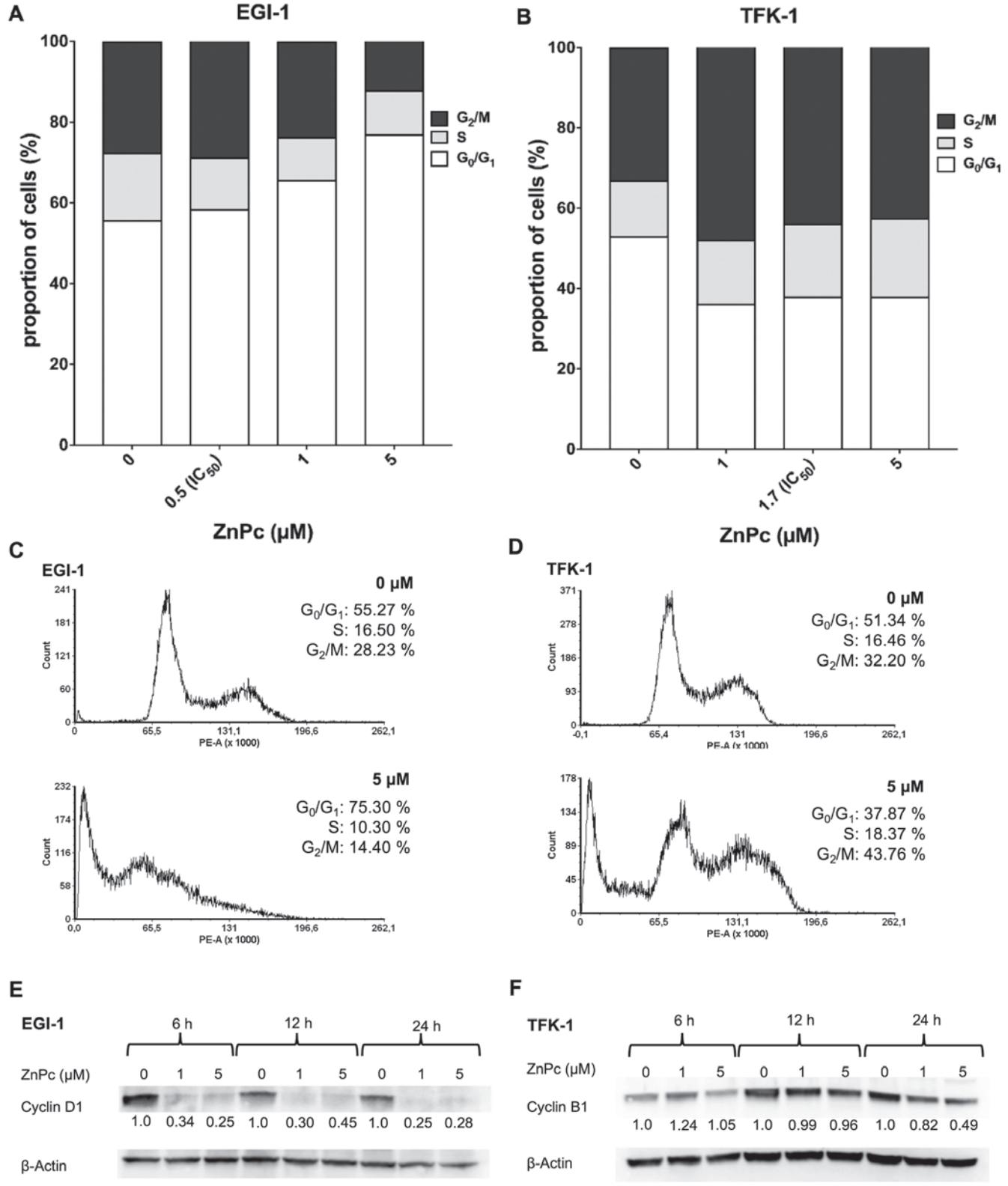

Figure 7. Effects of ZnPc-PDT on the cell cycle of cholangiocarcinoma cells. FACS analysis (A) proportions from the (C) output revealed a ZnPc-PDT-induced dose-dependent increase of EGI-1 cells in the G_0/G_1-phase, with a corresponding decrease of cells in the G_2/M-phase, at 24 h post-PDT. (E) Accordingly, the expression of Cyclin D1 decreased in a time- and dose-dependent manner. In TFK-1 cells, the FACS (B) proportions from the (D) output showed that ZnPc-PDT led to an increase of cells in the G_2/M-phase and decrease in the G_0/G_1-phase. (F) A pronounced decrease of Cyclin B1, in line with the observed cell cycle arrest, was observed in TFK-1 cells at 24 h. Results are representative of a minimum of three independent experiments. ZnPc, tetra-triethyleneoxysulfonyl substituted zinc phthalocyanine; Pc32, dihydroxy-2,9(10),16(17),23(24)-tetrakis(4,7,10-trioxaundecan-1-sulfonyl) silicon phthalocyanine; PDT, photodynamic therapy.

two cell lines (Fig. 2C and D) (38). As other second generation photosensitizers, including the clinically relevant 5-aminolevulinic acid, fail to induce permanent antiproliferative effects in gastrointestinal cancer (39), the findings in the present study showed the potential and advantageous suitability of ZnPc as a novel PS for PDT of CC.

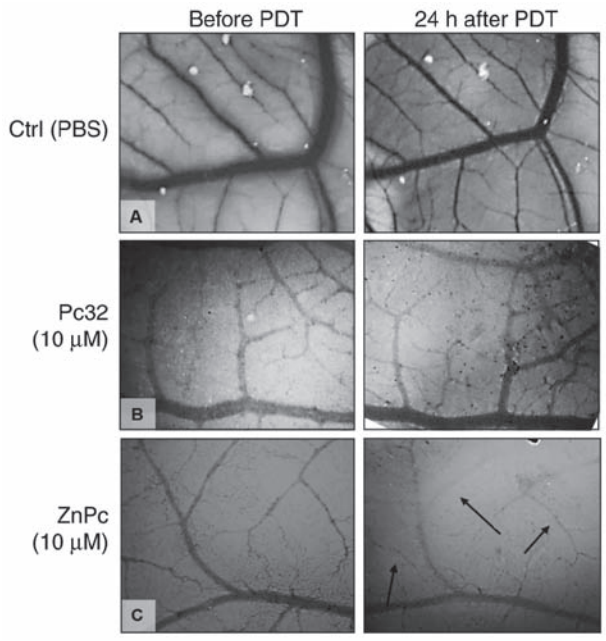

Figure 8. Blood vessel formation of the developing chicken chorioallantoic membrane (CAM) after ZnPc- or Pc32-PDT. Images show chicken CAMs in prior to and 24 h following PDT with (A) PBS (control), (B) Pc32 (10 μM) or (C) ZnPc (10 μM) as photosensitizers. In the control CAMs and in the Pc32-treated CAM, the vascular network was homogenous in arrangement in an antiparallel manner; after 24 h, new blood vessels had formed, as shown by branching of the small blood vessels. Only ZnPc-PDT induced a degeneration of the vascular network, shown as non-perfused regions and changes in branching of the small supplying vessels (arrows). Results are representative of three eggs per condition. Magnification, x12. CAM, chorioallantoic membrane; ZnPc, tetra-triethyleneoxysulfonyl substituted zinc phthalocyanine; Pc32, dihydroxy-2,9(10),16(17),23(24)-tetrakis(4,7,10-trioxaundecan-1-sulfonyl) silicon phthalocyanine; PDT, photodynamic therapy.

To determine whether there is a difference between silicon phthalocyanine and a zinc phthalocyanine on the growth reduction of CC, photoactivated Pc32 was used for comparison. Pc32 led to a time- and dose-dependent antiproliferative effect only in the less differentiated EGI-1 cells, but did not show comparable effects in the more differentiated TFK-1 cells. This finding is of importance, as other silicon-phthalocyanines have already been shown to induce potent antiproliferative effects in several different tumor entities, including gastrointestinal colon carcinoma cells (40), but have failed in CC cells. This underlines the importance of individually evaluating the potential of a PS in a specific tumor entity and shows that the findings in one tumor entity cannot easily be transferred to another.

Individual treatment-protocols, including light-dose, pre-incubation time and dose of PS, have an important influence on the clinical outcome, and differ from one cancer type to another (41-43). The time interval between the application of a PS and its subsequent photoactivation is essential for the subcellular uptake kinetics and distribution in a cancer cell. Fabris *et al* showed that incubation for 2 h was sufficient for a subcellular accumulation of a zinc phthalocyanine derivative in the golgi apparatus, whereas a more mitochondrial localization of this PS occurred only after 24 h (44). The present study evaluated the effect of different incubation times (10-24 h) on the effectiveness of the ZnPc-PDT in CC cells. PS loading for 24 h led to a more marked concentration-dependent antiproliferative effect of the subsequent PDT treatment, compared with shorter loading times of 10-16 h (Fig. 1C and D). After 10 h of PS loading, the PDT treatment induced significant antiproliferative effects only at high concentrations (>2.5 μM) of ZnPc. At concentrations <2.5 μM the effects were weak and the PDT-surviving CC cells tended to re-proliferate, which did not occur when the loading time was prolonged to 24 h. In a clinical setting, it can be beneficial to adapt the individual PDT-protocol for different CC entities, and identify a reasonable compromise between well-tolerated concentrations of PS with preferably low incubation times, but maintaining a sustained and pronounced antiproliferative effect of the PDT-treatment.

The efficacy of PDT on the target cells/tissue is determined by the photophysical properties of the PS, its uptake and the intracellular localization of accumulation (45,46). Investigations of other ZnPc and Pc32 derivatives have shown an accumulation of the PS in mitochondria, lysosomes and the golgi apparatus in various carcinoma cells (44,47-50). In the loading experiments performed in the present study, a predominantly cytoplasmic distribution of ZnPc was observed in the CC cells. However, marked generation of ROS was observed in the nucleus and mitochondria following PDT, suggesting there was also an appreciable accumulation of the photosensitizers in the nucleus, mitochondria or other organelles. These results are in line with our previous findings concerning the intracellular distribution and ROS-formation of ZnPc in gastrointestinal cancer cells, including esophageal cancer, indicating the phototoxic potency of photoactivated ZnPc and its preferred subcellular accumulation (23). The intracellular accumulation and formation of ROS were less pronounced with Pc32 following illumination than with ZnPc.

PDT-induced cell death is mediated via ROS formation, which can cause either necrosis and/or apoptosis (44). By measuring LDH release, a marked immediate cytotoxic effect of ZnPc-PDT was found in the two CC cell lines. Challa and Chan previously showed that increasing concentrations of extracellular LDH can indicate the primary necrosis of dying cells due to disturbance of cellular integrity. However, LDH release may also indicate the secondary necrosis of cells that have undergone apoptosis but are not taken up by phagocytosis under *in vitro* conditions (35,51). By contrast, Pc32-PDT did not lead to comparable cytotoxic effects in two cell lines. This observation supports the superiority of ZnPc in cellular uptake, ROS-formation and antiproliferative efficacy.

The inflammation-free elimination of cancer cells via apoptosis is a preferred therapeutic aim. Therefore, the present study also examined the apoptotic effects of ZnPc-PDT in the CC cells. It was shown that ZnPc-PDT induced mitochondrial-driven apoptosis with corresponding changes in the expression of regulatory proteins, Bax and Bcl-2. The expression of pro-apoptotic Bax increased, whereas the expression of anti-apoptotic Bcl-2 decreased, leading to a time- and dose-dependent increase in caspase-3 activity (Fig. 6). These data are in line with findings of Lam *et al,* who demonstrated the mitochondria-driven apoptosis of phthalocyanine-based PDT in epidermoid carcinoma cells (52) and Tampa *et al*, who elucidated that increasing levels of pro-apoptotic proteins and decreasing levels of anti-apoptotic proteins were the main apoptotic pathway in oral keratinocytes following zinc-sulphonated phthalocyanine-PDT (53).

The induction of cell cycle arrest at a specific cell cycle checkpoint by chemotherapeutic treatment is another mechanism to inhibit cancer cell proliferation in a non-inflammatory manner (54). Cell cycle arrest in the G_1- and G_2-phase can be induced by genotoxic compounds and ionizing radiation, which cause double stranded DNA breaks. In addition, S-phase arrest can be triggered by anti-metabolites, including 5-fluorouracil and hydroxyurea, whereas alkylating agents or topoisomerase-II-inhibitors can induce cell cycle arrest in the G_2-phase (55). In the present study, the concentration-dependent arrest of EGI-1 cells in the G_0/G_1-phase was observed 24 h following ZnPc-PDT, which was accompanied by a corresponding decrease of cells in the G_2/M-phase and a dose-dependent decrease in the expression of Cyclin D1 (56-58). In the more differentiated TFK-1 CC cells ZnPc-PDT also induced arrest in the G_0/G_1-phase, however, in contrast to the EGI-1 cells, the number of cells in the G_2/M-phase increased with an accompanied corresponding decrease in the expression of the G_2/M-phase-promoter Cyclin B1 (59). The data obtained on the cell cycle behavior of CC cells within various differentiation states offer valuable information for effective combination therapies, in which ZnPc-PDT is combined with chemotherapeutics to act at specific cell cycle phases in the future.

In addition to the described distinction in the induction of cell cycle arrest, the present study showed further differences between the two cell lines. PDT with either PS had a more marked and earlier antiproliferative effect on EGI-1 cells, compared with that on TFK-1 cells (Figs. 2 and 3). Correspondingly, higher immediate cytotoxicity (Fig. 5) and an earlier and more marked induction of apoptosis were observed in the EGI-1 cells (Fig. 6). The reasons for these variances between the two cell lines may lie in the individual differentiation of the two cancer cell lines and/or a dissimilar expression of regulatory proteins. The poorly differentiated EGI-1 cells (28,60) presumably overexpress p53, which is well known as an essential cellular protein, reacting to cell stress and DNA damage, and is involved in the regulation of cell cycle progression and apoptosis (61,62). By contrast, the partly papillary and partly tubular growing TFK-1 cells (29) lack marked expression of p53 (62). This indicates differences in the underlying mechanisms of PDT-induced cytotoxicity, and growth- and proliferation-inhibition in the context of cell line-specific genetic aberrations. It also supports the clinical need to perform PDT with an individual and PS-adjusted protocol, depending on the genetic characteristics, p53-status and differentiation of the individual type of CC.

At a certain size, the further growth of a solid tumor, including in CC, requires the formation of new blood vessels for the supply of oxygen and nutrients. Therefore, the development of novel anticancer compounds with antiangiogenic potency represents an attractive approach for future treatment strategies (63). Previous data show a correlation between microvessel density and reduced 5-year survival rates, higher recurrence rates and increased nodal spread in intrahepatic CC (64). Although ZnPc-PDT markedly inhibited neoangiogenesis and caused a degeneration of the vascular complex, as examined in the CAM assay of fertilized chicken eggs, no antiangiogenic and/or avascular effects were observed following Pc32-PDT.

Taken together, the results of the present study showed the suitability of the novel ZnPc for PDT of CC and its superiority compared with Pc32. Further investigations are required to examine the specific underlying mechanisms, particularly in the context of individual cancerous genetic alterations. Additionally, future investigations are required to examine the *in vivo* potency of the novel ZnPc-PDT in a monotherapeutic approach and in combination with clinically relevant chemotherapeutics.

Acknowledgements

Not applicable.

Funding

JS was supported by a scholarship of the Berliner Krebsgesellschaft e.V., Berlin. WK was funded by a scholarship of the Studienstiftung des Deutschen Volkes. RO was funded by the Humboldt Research Fellowship for Postdoctoral Researchers (Georg Foster Scholarship). GS was supported by a Ruth-Jeschke-Gedenkstipendium of the Charité-Universitätsmedizin Berlin.

Availability of data and materials

The datasets used and/or analyzed during the current study are available from the corresponding author on reasonable request.

Authors' contributions

JS and MH contributed to the conception and design of the research. JS, WK, RO, GS, JB and BH performed the experiments.AGG synthesized the PS used in this investigation. GN, BN, JS and MH analyzed the data. MH, BN and JS interpreted the results of the experiments. JS, GS, RO and WK prepared the figures. JS drafted the manuscript. JS, AGG, BN and MH edited and revised the manuscript. JS, WK, GS, RO, AGG, BN, GN, JB, BH, and MH approved the final version of the manuscript.

Ethics approval and consent to participate

Not applicable.

Consent for publication

Not applicable.

Competing interests

The authors declare that they have no competing interests.

References

1. Aljiffry M, Walsh MJ and Molinari M: Advances in diagnosis, treatment and palliation of cholangiocarcinoma: 1990-2009. World J Gastroenterol 15: 4240-4262, 2009.
2. Bergquist A and Von Seth E: Epidemiology of cholangiocarcinoma. Best Pract Res Clin Gastroenterol 29: 221-232, 2015.
3. Baradari V, Höpfner M, Huether A, Schuppan D and Scherübl H: Histone deacetylase inhibitor MS-275 alone or combined with bortezomib or sorafenib exhibits strong antiproliferative action in human cholangiocarcinoma cells. World J Gastroenterol 13: 4458-4466, 2007.

4. Doherty B, Nambudiri VE and Palmer WC: Update on the diagnosis and treatment of cholangiocarcinoma. Curr Gastroenterol Rep 19: 2, 2017.
5. Jarnagin WR, Fong Y, Dematteo RP, Gonen M, Burke EC, Bodniewicz BS J, Youssef BA M, Klimstra D and Blumgart LH: Staging, resectability, and outcome in 225 patients with hilar cholangiocarcinoma. Ann Surg 234: 507-517, 2001.
6. Ortner ME, Caca K, Berr F, Liebetruth J, Mansmann U, Huster D, Voderholzer W, Schachschal G, Mössner J and Lochs H: Successful photodynamic therapy for nonresectable. cholangiocarcinoma: A randomized prospective study. Gastroenterology 5085: 1355-1363, 2003.
7. Moole H, Tathireddy H, Dharmapuri S, Moole V, Boddireddy R, Yedama P, Dharmapuri S, Uppu A, Bondalapati N and Duvvuri A: Success of photodynamic therapy in palliating patients with nonresectable cholangiocarcinoma: A systematic review and meta-analysis. World J Gastroenterol 23: 1278-1288, 2017.
8. Ortner M: Photodynamic therapy in cholangiocarcinoma: An overview. Photodiagnosis Photodyn Ther 1: 85-92, 2004.
9. Abu-hamda EM and Baron TH: Endoscopic management of cholangiocarcinoma. Semin Liver Dis 24: 165-175, 2004.
10. Dolmans DE, Fukumura D and Jain RK: Photodynamic therapy for cancer. Nat Rev Cancer 3: 380-387, 2003.
11. Witzigmann H, Berr F, Ringel U, Caca K, Uhlmann D, Schoppmeyer K, Tannapfel A, Wittekind C, Mossner J, Hauss J and Wiedmann M: Surgical and palliative management and outcome in 184 patients with hilar cholangiocarcinoma. Ann Surg 244: 230-239, 2006.
12. Zoepf T, Jakobs R, Arnold J, Apel D and Riemann JF: Palliation of nonresectable bile duct cancer: Improved survival after photodynamic therapy. Am J Gastroenterol 100: 2426-2430, 2005.
13. Prasad GA, Wang KK, Baron TH, Buttar NS, Wongkeesong LM, Roberts LR, LeRoy AJ, Lutzke LS and Borkenhagen LS: Factors associated with increased survival after photodynamic therapy for cholangiocarcinoma. Clin Gastroenterol Hepatol 5: 743-748, 2007.
14. Lee TY, Cheon YK, Shim CS and Cho YD: Photodynamic therapy prolongs metal stent patency in patients with unresectable hilar cholangiocarcinoma. World J Gastroenterol 18: 5589-5594, 2012.
15. McCaughan JS Jr, Mertens BF, Cho C, Barabash RD and Payton HW: Photodynamic therapy to treat tumors of the extrahepatic biliary ducts. A case report. Arch Surg 126: 111-113, 1991.
16. Allison RR, Zervos E and Sibata CH: Cholangiocarcinoma: An emerging indication for photodynamic therapy. Photodiagnosis Photodyn Ther 6: 84-92, 2009.
17. Allison RR and Sibata CH: Oncologic photodynamic therapy photosensitizers: A clinical review. Photodiagnosis Photodyn Ther 7: 61-75, 2010.
18. Bonnett R: Photosensitizers of the porphyrin and phthalocyanine series for photodynamic therapy. Chem Soc Rev 24, 1995.
19. Josefsen LB and Boyle RW: Photodynamic therapy: Novel third-generation photosensitizers one step closer? Br J Pharmacol 154: 1-3, 2008.
20. Jiang Z, Shao J, Yang T, Wang J and Jia L: Pharmaceutical development, composition and quantitative analysis of phthalocyanine as the photosensitizer for cancer photodynamic therapy. J Pharm Biomed Anal 87: 98-104, 2014.
21. Neagu M, Constantin C, Tampa M, Matei C, Lupu A, Manole E, Ion RM, Fenga C and Tsatsakis AM: Toxicological and efficacy assessment of post-transition metal (Indium) phthalocyanine for photodynamic therapy in neuroblastoma. Oncotarget 7: 69718-69732, 2016.
22. Agostinis P, Berg K, Cengel KA, Foster TH, Girotti AW, Gollnick SO, Hahn SM, Hamblin MR, Juzeniene A, Kessel D, *et al*: Photodynamic therapy of cancer: An update. CA Cancer J Clin 61: 250-281, 2011.
23. Ochsner M: Light scattering of human skin: A comparison between Zinc(II)-phthalocyanine and photofrin II. J Photochem Photobiol B 32: 3-9, 1996.
24. Yslas EI, Prucca C, Romanini S, Durantini EN, Bertuzzi M and Rivarola V: Biodistribution and phototherapeutic properties of Zinc(II) 2,9,16,23-tetrakis (methoxy) phthalocyanine s. Photodiagnosis Photodyn Ther 6: 62-70, 2009.
25. Kuzyniak W, Ermilov EA, Atilla D, Gürek AG, Nitzsche B, Derkow K, Hoffmann B, Steinemann G, Ahsen V and Höpfner M: Tetra-triethyleneoxysulfonyl substituted zinc phthalocyanine for photodynamic cancer therapy. Photodiagnosis Photodyn Ther 13: 148-157, 2016.
26. Liu W, Chen N, Jin H, Huang J, Wei J, Bao J, Li C, Liu Y, Li X and Wang A: Intravenous repeated-dose toxicity study of ZnPcS2P2-based-photodynamic therapy in beagle dogs. Regul Toxicol Pharmacol 47: 221-231, 2007.
27. Atilla D, Saydan N, Durmus M, Gürek AG, Khan T, Rück A, Walt H, Nyokong T and Ahsen V: Synthesis and photodynamic potential of tetra- and octa-triethyleneoxysulfonyl substituted zinc phthalocyanines. J Photochem Photobiol A Chem 186: 298-307, 2007.
28. Scherdin G, Garbrecht M and Klouche M: In vitro interaction of á-difluoromethylornithine (DFMO) and human recombinant interferon-a (rIFN-a) on human cancer cell lines. Immunobiology 175: 1-143, 1987.
29. Saijyo S, Kudo T, Suzuki M, Katayose Y, Shinoda M, Muto T, Fukuhara K, Suzuki T and Matsuno S: Establishment of a new extrahepatic bile duct carcinoma cell line, TFK-1. Tohoku J Exp Med 177: 61-71, 1995.
30. Nitzsche B, Gloesenkamp C, Schrader M, Ocker M, Preissner R, Lein M, Zakrzewicz A, Hoffmann B and Höpfner M: Novel compounds with antiangiogenic and antiproliferative potency for growth control of testicular germ cell tumours. Br J Cancer 103: 18-28, 2010.
31. Cai Y, Xia Q, Su Q, Luo R, Sun Y, Shi Y and Jiang W: MTOR inhibitor RAD001 (everolimus) induces apoptotic, not autophagic cell death, in human nasopharyngeal carcinoma cells. Int J Mol Med 31: 904-912, 2013.
32. Gloesenkamp C, Nitzsche B, Lim AR, Normant E, Vosburgh E, Schrader M, Ocker M, Scherübl H and Höpfner M: Heat shock protein 90 is a promising target for effective growth inhibition of gastrointestinal neuroendocrine tumors. Int J Oncol 40: 1659-1667, 2012.
33. Höpfner M, Baradari V, Huether A, Schöfl C and Scherübl H: The insulin-like growth factor receptor 1 is a promising target for novel treatment approaches in neuroendocrine gastrointestinal tumours. Endocr Relat Cancer 13: 135-149, 2006.
34. Rodrigues JR, Charris J, Camacho J, Barazarte A, Gamboa N, Nitzsche B, Höpfner M, Lein M, Jung K and Abramjuk C: N'-Formyl-2-(5-nitrothiophen-2-yl)benzothiazole-6-carbohydrazide as a potential anti-tumour agent for prostate cancer in experimental studies. J Pharm Pharmacol 65: 411-422, 2013.
35. Krysko DV, Vanden Berghe T, D'Herde K and Vandenabeele P: Apoptosis and necrosis: Detection, discrimination and phagocytosis. Methods 44: 205-221, 2008.
36. Kuzyniak W, Schmidt J, Glac W, Berkholz J, Steinemann G, Hoffmann B, Ermilov EA, Gürek AG, Ahsen V, Nitzsche B and Höpfner M: Novel zinc phthalocyanine as a promising photosensitizer for photodynamic treatment of esophageal cancer. Int J Oncol 50: 953-963, 2017.
37. Mfouo-tynga I and Abrahamse H: Cell death pathways and phthalocyanine as an efficient agent for photodynamic cancer therapy. Int J Mol Sci 16: 10228-10241, 2015.
38. Roskoski R Jr: ERK1/2 MAP kinases: Structure, function, and regulation. Pharmacol Res 66: 105-143, 2012.
39. Höpfner M, Maaser K, Theiss A, Lenz M, Sutter AP, Kashtan H, von Lampe B, Riecken EO, Zeitz M and Scherübl H: Hypericin activated by an incoherent light source has photodynamic effects on esophageal cancer cells. Int J Colorectal Dis 18: 239-247, 2003.
40. Whitacre CM, Feyes DK, Satoh T, Grossmann J, Mulvihill JW, Mukhtar H and Oleinick NL: Photodynamic therapy with the phthalocyanine photosensitizer pc 4 of SW480 human colon cancer xenografts in athymic mice 1. Clin Cancer Res 6: 2021-2027, 2000.
41. Nanashima A, Isomoto H, Abo T, Nonaka T, Morisaki T, Arai J, Takagi K, Ohnita K, Shoji H, Urabe S, *et al*: How to access photodynamic therapy for bile duct carcinoma. Ann Transl Med 2: 23, 2014.
42. Oniszczuk A, Wojtunik-Kulesza KA, Oniszczuk T and Kasprzak K: The potential of photodynamic therapy (PDT)-experimental investigations and clinical use. Biomed Pharmacother 83: 912-929, 2016.
43. van Straten D, Mashayekhi V, de Bruijn H, Oliveira S and Robinson D: Oncologic photodynamic therapy: Basic principles, current clinical status and future directions. Cancers (Basel) 9: E19, 2017.
44. Fabris C, Valduga G, Miotto G, Borsetto L, Jori G, Garbisa S and Reddi E: Photosensitization with Zinc (II) phthalocyanine as a switch in the decision between apoptosis and necrosis. Cancer Res 61: 7495-7500, 2001.
45. Morgan J, Potter WR and Oseroff AR: Comparison of photodynamic targets in a carcinoma cell line and its mitochondrial DNA-deficient derivative. Photochem Photobiol 71: 747-57, 2000.
46. Oleinick NL, Morris RL and Belichenko I: The role of apoptosis in response to photodynamic therapy: What, where, why, and how. Photochem Photobiol Sci 1: 1-21, 2002.

47. Rodriguez ME, Zhang P, Azizuddin K, Delos Santos GB, Chiu SM, Xue LY, Berlin JC, Peng X, Wu H, Lam M, *et al*: Structural factors and mechanisms underlying the improved photodynamic cell killing with Silicon phthalocyanine photosensitizers directed to lysosomes v/s mitochondria. Photochem Photobiol 85: 1189-1200, 2012.
48. Tynga IM, Houreld NN and Abrahamse H: The primary subcellular localization of Zinc phthalocyanine and its cellular impact on viability, proliferation and structure of breast cancer cells (MCF-7). J Photochem Photobiol B 120: 171-176, 2013.
49. Shao J, Dai Y, Zhao W, Xie J, Xue J, Ye J and Jia L: Intracellular distribution and mechanisms of actions of photosensitizer Zinc (II)-phthalocyanine solubilized in Cremophor EL against human hepatocellular carcinoma HepG2 cells q. Cancer Lett 330: 49-56, 2013.
50. Biology C, Marino J, García MC, Furmento VA, Blank VC, Awruch J and Roguin LP: Lysosomal and mitochondrial permeabilization mediates zinc (II) cationic phthalocyanine phototoxicity. Int J Biochem Cell Biol 45: 2553-2562, 2013.
51. Challa S and Chan FK: Going up in flames: Necrotic cell injury and inflammatory diseases. Cell Mol Life Sci 67: 3241-3253, 2010.
52. Lam M, Oleinick NL and Nieminen A: Photodynamic therapy-induced apoptosis in epidermoid carcinoma cells. J Biol Chem 276: 47379-47386, 2001.
53. Tampa M, Matei C, Popescu S, Georgescu S and Neagu M: Zinc trisulphonated phthalocyanine used in photodynamic therapy of dysplastic oral keratinocytes. Rev Chim 64: 639-645, 2013.
54. Dickson MA and Schwartz GK: Development of cell-cycle inhibitors for cancer therapy. Drug Dev Contemp Oncol 16: 36-43, 2009.
55. Gabrielli B, Brooks K and Pavey S: Defective cell cycle checkpoints as targets for anti-cancer therapies. Front Pharmacol 3: 9, 2012.
56. Resnitzky D and Reed SI: Different roles for cyclins D1 and E in regulation of the G1-to-S transition. Mol Cell Biol 15: 3463-3469, 1995.
57. Gupta SC, Hevia D, Patchva S, Park B, Koh W and Aggarwal BB: Upsides and downsides of reactive oxygen species for cancer: The roles of reactive oxygen species in tumorigenesis, prevention, and therapy. Antioxid Redox Signal 16: 1295-1322, 2012.
58. Rezaei PF, Fouladdel S, Ghaffari SM, Amin G and Azizi E: Induction of G1 cell cycle arrest and cyclin D1 down-regulation in response to pericarp extract of Baneh in human breast cancer T47D cells. DARU 20: 101, 2012.
59. Su C, Lin J, Chen G, Lin W and Chung J: Down-regulation of Cdc25c, CDK1 and cyclin B1 and up-regulation of wee1 by curcumin promotes human colon cancer colo 205 cell entry into G2/M-phase of cell cycle. Cancer Gen Proteomics 3: 55-62, 2006.
60. Huether A, Höpfner M, Baradari V, Schuppan D and Scherübl H: Sorafenib alone or as combination therapy for growth control of cholangiocarcinoma. Biochem Pharmacol 73: 1308-1317, 2007.
61. Levine AJ: P53, the cellular gatekeeper for growth and division. Cell 88: 323-331, 1997.
62. Caca K, Feisthammel J, Klee K, Tannapfel A, Witzigmann H, Wittekind C, Mössner J and Berr F: Inactivation of the INK4a/ARF locus and p53 in sporadic extrahepatic bile duct cancers and bile tract cancer cell lines. Int J Cancer 97: 481-488, 2002.
63. Folkman J: Angiogenesis: An organizing principle for drug discovery? Nat Rev Drug Discov 6: 273-286, 2007.
64. Thelen A, Scholz A, Weichert W, Wiedenmann B, Neuhaus P, Gessner R, Benckert C and Jonas S: Tumor-associated angiogenesis and lymphangiogenesis correlate with progression of intrahepatic cholangiocarcinoma. Am J Gastroenterol 105: 1123-1132, 2010.